Water Motion and Sugar Translocation in Leaves

Tomas Bohr, Hanna Rademaker and Alexander Schulz

Abstract We give an overview of the current understanding of the coupled water—and sugar flows in plants with special emphasis on the leaves. We introduce the Münch mechanism and discuss the particularities of osmotically driven flow in the phloem and the consequences for the allometry of the vasculature. This is first done in the context of the entire tree, where we discuss the optimum radius for the phloem tubes, and later for a single needle, where we give a more detailed solution of the osmotic flow profile, allowing us to understand the constraints on needle sizes. We then discuss recent results from microscopy of cross sections along the midvein of a birch leaf, allowing us to measure how the number and radius of the sieve elements depend on the distance from the petiole and compare this to the available area and the minor vein endings in the entire leaf. We finally discuss the pre-phloem water flow in the leaf, i.e. the coupled water/sugar transport from the mesophyll via the bundle sheath into the sieve tubes. We review the distinct sugar loading mechanisms with special emphasis on active symplasmic loading ('polymer trapping'), where one needs to compute water and sugar flow through extremely narrow channels.

Introduction

The ability to provide water for all vital parts is crucial for the survival of a plant. The predominant solvent in all cells is water, which allows intescellular transport by diffusion or through membrane proteins. In addition, plants depend upon water for transpiration, for photosynthesis and for transport of photosynthates—mainly sugars. Since water is predominantly taken up in the roots and sugars are produced in the leaves, the plant has a great need of long-distance translocation of sap—water with solutes—and thus for a vascular system. The vascular system basically consists

T. Bohr (✉) · H. Rademaker
Department of Physics, Technical University of Denmark, 2800 Kgs, Lyngby, Denmark
e-mail: tomas.bohr@fysik.dtu.dk

A. Schulz
Department of Plant and Environmental Sciences, University of Copenhagen, Copenhagen, Denmark

A. Geitmann and J. Gril (eds.), *Plant Biomechanics*,
https://doi.org/10.1007/978-3-319-79099-2_16

of two parts, the *xylem* and the *phloem*, as sketched in Fig. 1, and although the driving mechanisms for the flow in these two strongly interconnected circuits are completely different, they both are activated by the leaves. See, e.g. Taiz and Zeiger (2010)) for a thorough introduction to the vascular system of plants and (Jensen et al. 2016) for a recent review of the physics of sap-translocation.

The fact that plants, through transpiration from the leaves, reemit most of their precious water uptake is quite surprising, but the acquisition of CO_2, which occurs by diffusion from the surrounding air through the stomata in the leaf surface, inevitably causes great water loss due to the small concentration of CO_2 in the air and the large water concentration (essentially 100% humidity) in the leaf. This creates a need for large flows from the roots up to—and through—the leaves, which takes place in the tracheids and vessels of the xylem. This flow is believed to be mainly driven by suction in the leaves—a surprisingly strong suction. The direct measurement of pressures inside leaf cells is extremely difficult, due to the seemingly unavoidable issues of leakage at such strong suction rates; but results from pressure bombs (Taiz and Zeiger 2010) indicate that leaves are able to create extremely low pressures (or indeed large suctions, since these pressures are well below zero) down to, say, −80 bar (−8 MPa). Both the generation of these large suction rates and the dependability

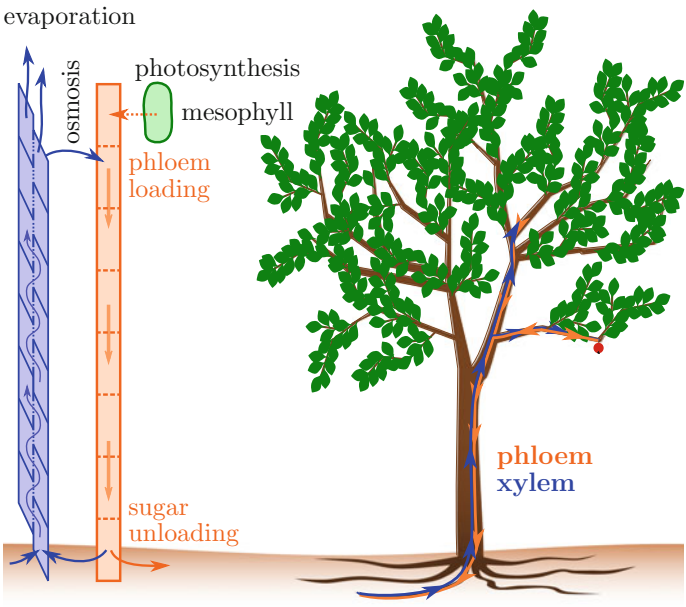

Fig. 1 The vascular system of a plant consists of two parts—the *xylem* transports water from the roots up to the leaves, where most of the water is evaporated. A fraction of the delivered water is used in photosynthesis inside the green mesophyll cells. Another portion is used to drive the flow in the other part of the vascular system—the *phloem*, which distributes the sugars produced in photosynthesis to other parts of the plant, e.g. roots, growing shoots and fruits

of such obviously unstable flows are not well understood. The mechanism for the generation of negative pressures is usually explained in terms of surface tension, i.e. capillary rise in extremely narrow (nanometric) pores between the cell walls of the mesophyll cells (Taiz and Zeiger 2010). It is probably more likely that it is the gelatinous polymers, e.g. the pectins, which provide the water suction, and thus that the cell wall structure is of paramount importance, as it is for growth of the leaves (see, e.g. Jensen et al. 2016 for a discussion). For the stability of the flow in the xylem, the organization of the tubes (vessels and tracheids) through which it travels is very important. These tubes are laterally connected and the flow moves between them through the so-called pits—valves that close if an embolism (an air bubble) occurs, thereby preventing the air from spreading.

The other part of the vascular system, the phloem, is quite different on almost all counts. The flow volume in the sieve tubes of the phloem is an order of magnitude smaller, it contains photosynthates in concentrations up to about 1 M, and the sap flows under positive pressure, generated by osmosis, stealing the water out of the xylem. The so-called Münch hypothesis explains the flow as caused by the loading of sugars into the sieve tubes in the minor veins in mature leaves, which generates a large osmotic pressure. Similarly, sugars are released from the sieve tubes in the roots, whereby the osmotic pressure becomes lower. The result is a pressure difference of up to around 10 bars (1 MPa) driving the flow, corresponding to a concentration difference of around 0.5 M. The phloem tubes in the stem of a tree of height, say, $H = 50$ m have a typical radius $a \approx 20\,\mu$m and the sap viscosity η is about twice that of water, i.e. $\eta = 2 \times 10^{-3}$ Pa s. With these values, we can estimate a typical flow velocity in a cylindrical phloem (sieve) tube with stationary Poiseuille flow:

$$u \approx \frac{a^2}{8\eta H}\Delta p \approx 5 \times 10^{-4}\ \text{m/s} \approx 180\ \text{cm/h}, \tag{1}$$

which corresponds reasonably well to measured flows, being on the high side. In fact, the sieve plates that separate the individual sieve 'elements' (or sieve cells) contribute a friction which effectively doubles the viscosity (Jensen et al. 2012c). Also, there are significant differences between angiosperms (broad-leaved trees) and gymnosperms (conifers), whose flows are slower (Liesche et al. 2015). So although it seems counter-intuitive that osmotic pressure differences between leaves and roots in a 50 m high tree can generate the measured flows, actual measurements of flow rates, concentrations and the diameters of the sieve tubes indicate that this is indeed feasible (Jensen et al. 2016). In particular, there is an indirect, but quite strong, argument coming from the allometry of the phloem vascular system (Jensen et al. 2011). Indeed, the osmotic flows generated in the leaves would predict a specific scaling of the typical sieve tubes radius a with the height H of the stem and the length l of the leaves. One has to remember that the flow is generated in the leaves, by osmotic water uptake across the surface of the sieve tubes, whereas the resistance to the flow mainly comes from the stem as in (1). Modelling the phloem as long tubes going from leaf to root without change of radius, one can ask what the optimal radius a^* would be, that is, the radius which makes the flow velocity largest (Jensen et al.

2016). If the radius is very small, the osmotic 'pump' in the leaf is very efficient, since the surface to volume ratio of the tube is large; but the resistance through the stem also becomes large since the tube is narrow. On the other hand, if the radius is large, the resistance through the stem is small, but now the osmotic pump is less efficient. In conclusion, we might expect an optimum somewhere in between.

To investigate this quantitatively, we can, following (Jensen et al. 2012b, 2016), represent the different elements of the tube as resistors, yielding a certain velocity, when a certain pressure difference is applied. For the stem, the relation would be given by (1), with Δp representing the pressure drop Δp_s from top to bottom of the stem, but for the leaves, the relation would be very different: The flux would be proportional to the *surface area* $2\pi al$. Dividing by the tube cross section πa^2, the velocity would be

$$u \approx \frac{2l}{a} L_p \Delta\pi_l, \tag{2}$$

where L_p is the membrane conductance or permeability (pr. unit area), and $\Delta\pi_l$ the osmotic pressure difference between the inside and the outside of the tube, namely $RT\Delta c$, where Δc is the (sugar) concentration difference across the tube membrane. Since the velocities in the leaf and the root should be the same, occurring in the same tube, the pressures are related by

$$\frac{\Delta\pi_l}{\Delta p_s} \approx \frac{a^3}{16\eta L_p l H} \tag{3}$$

and, as one can easily verify, the largest velocity is achieved when this ratio is 2 which determines an optimal tube radius

$$a^* = (2H\, l\, l_{\mathrm{m}})^{1/3} \tag{4}$$

i.e. the cube root of the product of three lengths: the height of the tree, the length of the leaves and a 'membrane length' $l_{\mathrm{m}} = 16\eta L_p$. In Fig. 2a, we show this prediction compared with data from field measurements on a broad range of plants—with heights from 10 cm to 50 m, and as one can see, they compare reasonably well. Here, a geometrical factor G is included (Jensen et al. 2012b) taking into account the non-cylindrical cross section of some sieve tubes (especially in conifers), and a is thus also an effective radius, $a = \sqrt{A/\pi}$.

One might speculate why the roots were not included in the analysis, when, in fact, they play a role very similar to the leaves, just unloading sugar and water instead of letting them in. Thus, the length of the roots should also appear in (4). As one can easily verify (Jensen et al. 2016), the inclusion of a root section with length l_r would simply change the l appearing in (4) to $(l^{-1} + l_r^{-1})^{-1}$ and the result we gave above was actually valid for the case $l \ll l_r$, which is the case for most trees. One can also note the very small value of the 'membrane length' l_{m}. For typical sieve tube membranes, the permeabilities are very small and $\eta L_p \approx 10^{-16}$ m. One should, however, not think of this as a length. If we think of the pores in the membranes as

narrow channels of radius a_p, length (thickness of the membrane) d and covering fraction ϕ, we would find

$$\eta L_p \sim \frac{\phi a_p^2}{d} \tag{5}$$

and with $d \approx 5\,\text{nm}$, $\phi \approx 10^{-4}$ we find such values for ηL_p, when a_p is of the order of an Ångström, which corresponds to the size of the aquaporins that transport the water. As a final comment of the scaling relation, one might note that it is the *velocity* of the phloem, not the *flux*, which is maximized. One can easily verify that the fluxes, obtained by multiplying the velocities in (1) and (2) by the cross section πa^2 would not have a maximum for any finite a, but would increase without bounds with a. If, as is more realistic, we fix the total cross-sectional area available for transport, we do get maximal flux for the a^* predicted above.

Another interesting size scaling relates the radius of the sieve tubes to the height of the tree. As shown in Fig. 2b, this radius, or, more precisely the cross-sectional area A which is preferred since the tubes are not all cylindrical, increases with height for small plants, but at a height of around 10 m it saturates at a value corresponding to a tube radius of around 20 µm. The reason for this is currently unknown, but since each section of the sieve tube (the sieve tube element) is a single cell, there might be good architectural reasons for not increasing its size.

An interesting corollary of the size scalings of Fig. 2a, b is brought out in Jensen and Zwieniecki (2013), where it is shown that large trees have small leaves. Indeed, if the sieve tubes of large trees are fixed at $a \approx 20\,\mu\text{m}$, and these radii are also optimal as in (4), the leaf length l and the tree height must be linked as $l \sim 1/H$. There could of course be other reasons why tall trees have small leaves, e.g. the increased wind

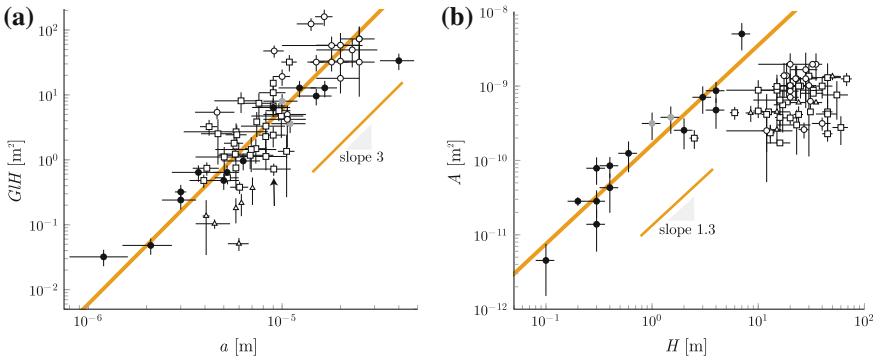

Fig. 2 **a** The optimal sieve tube radius (a^*) versus the values of the sieve tube radii from field measurements in mature stems of angiosperm herbs (solid circles), angiosperm trees (open circles), angiosperms shrubs (grey circles), gymnosperm trees (open squares) and gymnosperm trees with scales (open triangles). G is geometrical factor taking into account the non-cylindrical cross section of some sieve tubes (Jensen et al. 2012b). **b** Sieve tube cross-sectional area $A \approx \pi a^2$ as function of the height H of the tree. From Jensen et al. (2012b)

shear at higher altitudes. The more conventional arguments describing the mechanical constraints on leaf sizes are given in the classical text by Niklas (1994).

The Münch hypothesis has recently been tested directly on living plants (Knoblauch et al. 2016). Measuring the pressure directly in sieve tubes of the vine 'Morning Glory', it was verified that the pressure differential between the lowest leaves and the roots was sufficient to drive the flow, and that it increased for older plants, where these leaves were at a larger height. Interestingly enough this pressure differential does not grow linearly with height, but the plant compensates by the increased conductivity of the growing sieve tubes.

The scaling described above (represented by (4)) is based on the simplistic model of a tree as a collection of uniform tubes, which of course is very unrealistic. The radii for the sieve tubes of trees appearing in Fig. 2 were measured on mature plants, typically at a height of 1.3 m. In leaves, the sieve tube radii are actually considerably smaller, and in the veins of broad leaves, with a hierarchical venation pattern, the number of sieve tubes increases from order to order while their size decreases (Carvalho et al. 2017a, b). How, or whether, this can lead to a resistance proportional to the leaf length l as used in the simple model, is currently not understood.

The efficiency of the osmotically driven flows in the phloem depends on the leaves' ability to load sugars into the sieve elements of the minor veins and transport it away rapidly. For this, the vein architecture as well as the 'loading strategy' is of major importance. In the following, we shall review the current understanding of the flow of sugar in the leaf, from the mesophyll cells to the petiole. We shall start with the flow in the veins, and discuss two cases: first the flow in a leaf with a linear architecture—a conifer needle—and second, the architecture and flow of a birch leaf. Then, we shall discuss the pre-phloem pathway—from the mesophyll, through the bundle sheath and into the sieve tubes—with particular emphasis on the role of the water.

The Simplest Osmotic Flows with Conifer Needles as Example

We shall start with a somewhat more detailed picture of an osmotic flow. Instead of trying to model the entire tree, we shall focus only on the leaf-part, and only do that in the simplest possible configuration, which is a linear leaf like a conifer needle. Typically, there are one or two vascular bundles at the centre of the needle cross section, running from tip to petiole (Fig. 3). There is no hierarchical branching structure as in many broad leaves (see section "The Architecture of Broad Leaves"). Ronellenfitsch et al. (2015) measured the numbers and radii of sieve elements in needles of four conifer species. For their study, they chose needles of very different lengths, ranging from 1 to 35 cm. In all four species, they found the radius of the sieve elements to be almost constant from tip to base. They further found the number of sieve elements to increase from tip to base in a square-root shape, where most of the sieve elements start already close to the tip of the needle. Based on these findings,

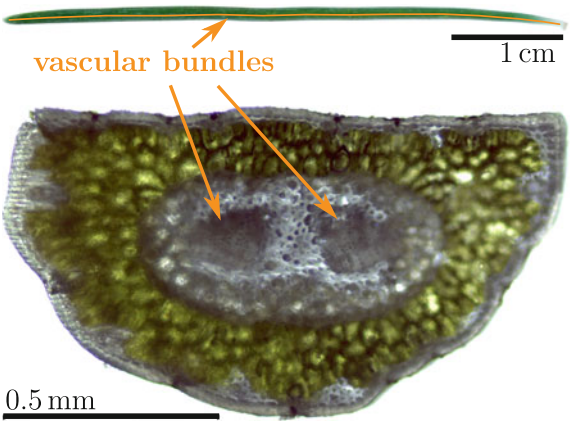

Fig. 3 Linear, unbranched venation in needles. Outside view and cross section of a conifer needle with two vascular bundles. The vascular bundles, and the conducting sieve tubes within, are running all the way from the tip to the base of the needle. The green cells surrounding the vascular bundles are sugar-producing mesophyll cells. From Rademaker et al. (2017)

we model a conducting tube as a single, unbranched conduit of the same length as the needle. We shall show that this way of modelling will allow us to understand why needles are quite restricted in length compared to broad leaves.

As discussed above, osmotic flows are driven by the concentration differences of solutes (mostly sugars) across the semipermeable membranes of the tubes. We shall assume that the plant is able to uphold a constant concentration difference between the inside and the outside of the tube—using one of the sugar loading mechanisms described in section "Water Flow Inside the Leaf". As a consequence, water is drawn in from the surroundings and creates a net axial flow as indicated in Fig. 4. In this case, the direction of the flow is from left to right, since we are assuming an impenetrable wall at $x = 0$, corresponding to the tip of the needle. As explained in detail in Jensen et al. (2016), such flows are well described by the so-called Münch-Horwitz equations, in terms of only the mean axial velocity u, the mean concentration c and pressure p. For *stationary flows*, to which we shall restrict our attention in the following, the Münch-Horwitz equations are: first, the osmotic water uptake, for a tube of fixed radius a and membrane permeability L_p, giving the incremental change in fluid flux $Q(x)$ along the tube in terms of the water potential difference $\Delta\Psi$ across the membrane surface as

$$dQ = L_p dA \Delta\Psi = L_p dA(RTc(x) - p(x)), \tag{6}$$

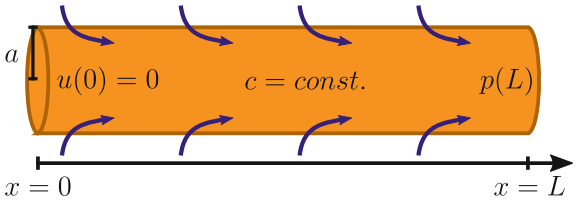

Fig. 4 The simplest osmotic flow. In the context of a conifer needle, $x = 0$, where the flow begins, is the tip and the outlet $x = L$, where the pressure prescribed would be the base

where $c(x)$ and $p(x)$ are *differences* between the concentrations and pressures inside and outside the tube and $dA = 2\pi a dx$ is the differential surface area. This means that the axial velocity satisfies

$$\frac{du}{dx} = \frac{1}{\pi a^2}\frac{dQ}{dx} = \frac{2L_p}{a}(RTc(x) - p(x)), \tag{7}$$

The second equation is Darcy's law (for a Hagen–Poiseuille flow), relating the pressure gradient to the velocity through the viscosity η of the fluid

$$\frac{dp}{dx} = -\frac{8\eta}{a^2}u(x). \tag{8}$$

These equations should be complemented by an equation for the sugar loading, the reaction–diffusion equation

$$\frac{d(uc)}{dx} = D\frac{d^2c}{dx^2} + \Upsilon(x), \tag{9}$$

defining the loading function $\Upsilon(x)$. In the following, we shall, however, following (Rademaker et al. 2016), assume that the loading is able to keep the concentration $c(x)$ constant $= c_0$ throughout the tube. This does not seem far from the situation in many plants and it is close to the situation obtained from 'target concentration' models (Jensen et al. 2012a). It can further be shown (Rademaker et al. 2016) that this choice of $c(x) = c_0$ is *optimal*, in the sense that no concentration profile, limited everywhere by the value c_0, can generate larger flows. If we are interested in limits to sap flow efficiency this simplification is thus relevant. Differentiating (7) and inserting (8) we find

$$\frac{d^2u}{dx^2} = -\frac{2L_p}{a}\frac{dp}{dx} = \frac{16\eta L_p}{a^3}u(x) \tag{10}$$

and introducing the characteristic length

$$L_{\text{eff}} = \frac{a^{3/2}}{(16L_p\eta)^{1/2}} = \frac{a^{3/2}}{l_{\text{m}}^{1/2}}, \tag{11}$$

we can write (10) as

$$\frac{d^2u}{dx^2} = \frac{1}{L_{\text{eff}}^2}u(x) \tag{12}$$

which indicates an exponential behaviour as $e^{\pm x/L_{\text{eff}}}$. In fact, when $u(x = 0) = 0$, the solution is

$$u(x) = A\sinh\left(x/L_{\text{eff}}\right). \tag{13}$$

The fact that there exists a characteristic scale L_{eff} different from the length L of the tube is very important. Their ratio can be expressed in terms of the dimensionless Münch number (Jensen et al. 2016)—the ratio of axial resistance in the tube and radial resistance through the surface.

$$M = \frac{16\eta L_p L^2}{a^3} = \frac{L^2}{L_{\text{eff}}^2}. \tag{14}$$

That the length scale L_{eff} plays a special role was first pointed out by Landsberg and Fowkes (1978) in the context of water uptake in the roots. In this case, the concentration is practically zero, and thus, the roots are dragging in water, mostly through suction generated by the negative pressures in the leaves. Since the concentration c_0 does not appear in (12), the same equation holds.

The flow profile along a tube, which is formed by chains of sieve cells in gymnosperm needles, strongly depends on $L_{\text{eff}}/L = 1/\sqrt{M}$. In Fig. 5, we show the velocity profile along the tube for three values of L_{eff}/L. For tube lengths not much larger than L_{eff}, the velocity grows linearly along the tube, but for long tubes (where L_{eff}/L is small), it becomes strongly non-linear. In fact, it almost vanishes near the tip and only reaches appreciable values in a region of the order of L_{eff} near the base. For a pine needle, a large value of M would thus not be very good. As shown in the lower curve in Fig. 5, a large region of the tube near the tip ($x = 0$) would be stagnant, and the sugar produced there would never get to the outlet.

The flow at the outlet $x = L$ (the base of the needle) is similarly found as Rademaker et al. (2016)

$$u(L) = \frac{1}{2}\sqrt{\frac{rL_p}{\eta}}\,(RTc_0 - p(L))\tanh\frac{L}{L_{\text{eff}}}, \tag{15}$$

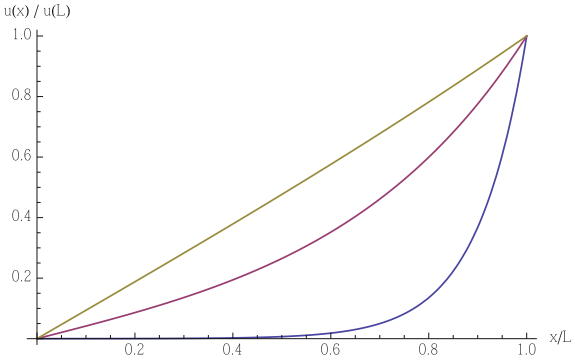

Fig. 5 The velocity profile along the tube formed by continuous sieve cells in a needle for three values of L_{eff}/L: 1.4 (top, yellow), 0.4 (middle, red) and 0.1 (bottom, blue). The tip of the needle would be towards the left at $x = 0$ and the base to the right at $x = L$. For large Münch numbers M (bottom curve), a zone of stagnant fluid forms at the tip of the needle

where $p(L)$ is the specified pressure at the outlet. For long tubes (i.e. large M), this approaches

$$u(L) = \frac{1}{2}\sqrt{\frac{rL_p}{\eta}}\,(RTc_0 - p(L)) \tag{16}$$

which is *independent* of L.

This result does of course depend on the assumption that the sugar concentration is constant in the tube. If the conifer could increase the concentration near the needle tip, larger pressures could build up and the sap would start to flow. But there must be a limit to the concentration a given species is able to build up. If we call that concentration c_0, then one can show (Rademaker et al. 2017) that the largest exit velocity is generated for the situation, where $c(x) = c_0$ along the whole tube. So, e.g. for the lowest curve (with $L_{\text{eff}}/L = 0.1$) the exit velocity is limited by (16) even if parts of the tube have a lower concentration. The exit velocity will thus not increase with L. This would mean that a needle would not gain much in sugar transport by making its needles longer than L_{eff}, so if no other concerns (e.g. competition for sun or elastic properties) are equally important this length should limit needle sizes. In fact, as shown in Fig. 6, the distribution of needle lengths seems roughly exponential with 75% of needles no longer than 6 cm in accordance with the value of L_{eff}. There could of course be other reasons, why long needles would not be optimal, e.g. their ability for self-support (Tadrist and Darbois-Texier 2016). Also, it would be very interesting to know how the 25% of species with longer needles have dealt with the flow limitations described above.

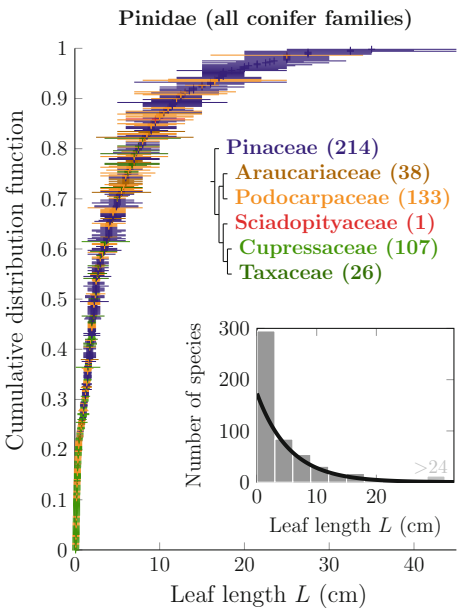

Fig. 6 The distribution of needle lengths of 519 conifer species. 75% of needles are no longer than 6 cm. Longer needles might be disadvantageous because of the formation of a stagnant zone in needles longer than L_{eff}, as predicted by Eq. 11 From Rademaker et al. (2017)

The Architecture of Broad Leaves

Leaves have two tissue types that are relevant for understanding the movement of water and sugars: mesophyll tissue and vascular tissue. Mesophyll cells contain chloroplasts and are therefore able to do photosynthesis to produce sugars. These sugars are then transported towards the vascular tissue, the veins, and taken up into the phloem tissue inside the veins. The main functions of the vascular tissue are mechanical stability and transport. Here, we will concentrate on the transport function.

A typical spatial arrangement of mesophyll and vascular tissue can be seen in Figs. 7 and 8. A dense layer of mesophyll cells at the upper side of the leaf supports the optimal absorption of sunlight for photosynthetic activity. The spongy arrangement of mesophyll cells towards the lower side of the leaf enables optimal gas exchange with the surrounding air spaces, securing sufficient supply of carbon dioxide. Embedded in these green cells are the veins, which are enclosed by a single layer of bundle sheath cells, shielding the vein from the surrounding air spaces.

Inside the veins are several cell types, two of which are directly relevant to transport: first, the large water-conducting vessels of the xylem and second, the thick-walled sieve elements of the phloem, responsible for the distribution of photosynthates and signalling molecules. The mature vessels are dead cells, which reduces the resistance to flow; and even in sieve tubes, which are living cells, only few organelles are present. This makes them dependent on neighbouring companion cells, to which they have numerous symplasmic connections, the so-called plas-

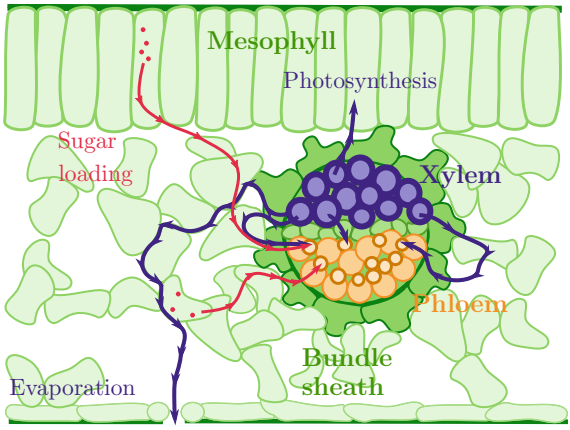

Fig. 7 Leaf cross section showing phloem and xylem conduits inside the vein, enclosed by the bundle sheath, which protects the vascular bundle from air. The surrounding mesophyll cells produce sugars (red) in photosynthesis, which are then transported towards the vein and loaded into the phloem. Water (blue) from the xylem is mostly evaporated through stomatal pores on the lower side of the leaf. A small portion of the water is used in photosynthesis and to drive the flow in the phloem

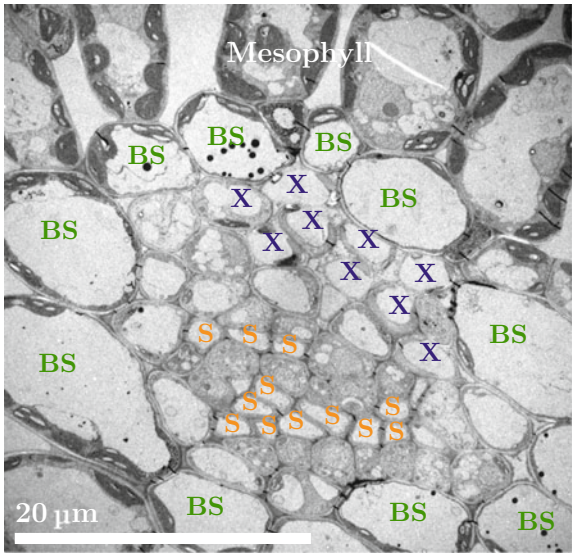

Fig. 8 Transmission electron microscopy image of a vein cross section, taken from an apple (*Malus sylvestris*) leaf. The image shows the xylem vessels (X) and the sieve elements (S) of the phloem inside the vein. A layer of bundle sheath (BS) cells encloses the vein and shields it from the surrounding air spaces. See also Fig. 7

modesmata. It is through these plasmodesmata that the sieve cells are supplied with substances they cannot produce themselves. Companion cells also play an important role in sugar loading, the process of taking up sugars into the phloem (see section "Water Flow Inside the Leaf").

Veins are organized in a hierarchical manner, where the largest (or *first order*) vein is the continuation of the vascular tissue in the petiole. Veins branching off from the first-order vein are called second-order veins and so forth, until the smallest veins. Veins of order one, two and three are also called *major veins*, whereas the higher order veins are called the *minor veins*. Release of water and uptake of sugars takes place mainly in the minor veins, while the function of the major veins is thought to be mostly transport and mechanical stability. The hierarchical organization allows for efficient access to the minor veins from the whole leaf blade (Fig. 9). Leaves of different species show different vein branching patterns. Understanding what makes these patterns optimal has been strongly debated (see, e.g. Jensen et al. 2016 and the references therein). However, there are only few studies addressing the inner structure of veins—in particular the relatively small part belonging to the phloem. The two basic parameters related to transport are the *number* of conduits and their *radius*. Conduits with smaller radius have a larger surface area to volume ratio. Since the release and uptake of water and sugars happen at the cell wall, we would expect the conduits inside minor veins to have smaller radii than inside major veins and a much greater number. Recently, these important parameters were carefully measured for leaves of poplar (Carvalho et al. 2017b) and of gingko (Carvalho et al. 2017a). In poplar, which has a classical hierarchical venation pattern bifurcating from the midvein towards the edge of the leaf it was found that the radii of the individual sieve elements decrease from the petiole to the 7th order veins by roughly a factor of 3,

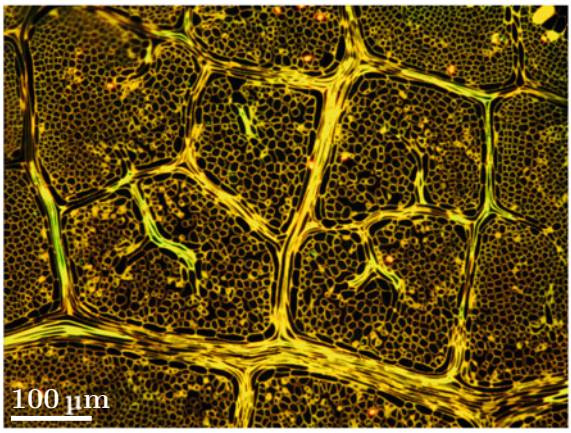

Fig. 9 Paradermal section of a young, fixed birch leaf stained with the fluorescent dye Coriphosphine O. The image shows veins of different orders from the smallest minor veins to a third-order vein. The veins are surrounded by mesophyll cells

whereas the total cross-sectional area (not surface area) of sieve elements *increases* roughly exponentially with order.

Our own study on birch leaves (Rademaker 2016) shows similar behaviour. Analysing ten cross sections along the midvein of a birch leaf, this study found that the radius of sieve tubes in the petiole is about twice as large as at the tip of the leaf ((1.9 ± 0.6) µm vs. (1.0 ± 0.2) µm), where the midvein is almost reduced to the size of a minor vein ((0.7 ± 0.2) µm). Looking at cross sections of minor veins, we found on average three sieve elements per smallest minor vein. The total number of minor vein endings per birch leaf was estimated from pieces of cleared leaves (Martens 2017). These two informations combined lead to an estimate of about 150,000 sieve elements in total in all minor vein endings of one leaf. Comparing this with the approximately 570 sieve elements found inside the petiole shows a massive (roughly 260-fold) reduction in the number of sieve tubes from minor to major veins. Moreover, the total cross-sectional area of sieve elements measured at points along the midvein, was found to increase from tip to base, correlating closely with the blade area of the part of the leaf, which would be expected to export sugar through this point (i.e. the leaf area measured from the point on the midvein, where the section was taken, to the tip of the leaf, choosing the boundary parallel to the second-order veins).

Water Flow Inside the Leaf

As discussed in the previous section, the leaves are the endpoint of the long-distance transport of water in the xylem and the starting point of the long-distance transport of sugars from the site of their production in the mesophyll to the site of consumption and storage in the sink organs of the plant, such as roots, immature leaves and reproductive organs (flowers and cones). Significantly, the leaves also provide the

main driving force for both, xylem and phloem transport. We will first consider the pathway of water from the xylem through the cell wall and air space in the leaf to the stomata, which regulate the rate of evaporation, and then the opposite pathway of sugars from the mesophyll cells via the bundle sheath to the phloem as sketched in Fig. 7. When discussing transport in the leaf one distinguishes between two basic pathways: symplasmic and apoplasmic. The symplasmic pathway goes through the interior of the cells via plasmodesmata, while the apoplasmic pathway is on the outside of the cells, through the cell walls. While the water, after leaving the xylem, is spreading out to different destinations—to be evaporated from the apoplast, to enter photosynthesis in the mesophyll and to enter the phloem osmotically—the sugar transport from the mesophyll cells is merely funnelled into the phloem. One can think of the water going into the phloem as a turning point of water flow in the vascular water circulation. While sugars follow a one-way path from source to sink, water circulates in the phloem back to the root where it is released from the phloem to travel up in the xylem together with freshly acquired water up to the leaves again.

Transpiration and Stomata

After exiting the xylem vessels, water might stay in the apoplast or enter the living cells and diffuse symplasmically. Apoplasmic water can follow the cell wall contacts via the bundle sheath into the mesophyll from which it can evaporate into the large intercellular air spaces (Fig. 10). The cell wall material consists of a number of different carbohydrates, the most important of which are cellulose, hemicelluloses and pectins. Those parts are hydrophilic and able to bind water molecules strongly. Water release from leaves takes a phase transition from liquid to vapour at the interface of cell walls and air spaces inside the leaf, and is controlled by a large number of stomata, openings that connect the internal air spaces with the environment. Each stomatal opening is controlled by a pair of guard cells which are able to respond to internal and environmental cues such as plant hormones, light conditions and CO_2 concentration. Their increase in volume opens stomata, while shrinkage closes them. The leaf surface is covered by a lipophilic (hydrophobic) layer and does not contribute to the evaporation (Lu et al. 2012).

In terms of biomechanics, the collection of stomatal openings act as a resistor for evaporation—and thus for water transport from roots to leaves—and limits at the same time the uptake of CO_2 through these openings which again limits photosynthesis. According to textbook knowledge, the driving force for transpiration is the difference in water vapour concentration between the leaf air spaces and the external air. This again is regulated by the diffusional resistance of the pathway through the stomatal openings. These values, though different for plants adjusted to different environments, can easily be quantified. By contrast, it is difficult to estimate the share of water that takes the apoplasmic pathway and evaporates compared to the two others: the share that is taken up by mesophyll cells for photosynthesis and the share that is osmotically taken up by the phloem directly and enters circulation. For

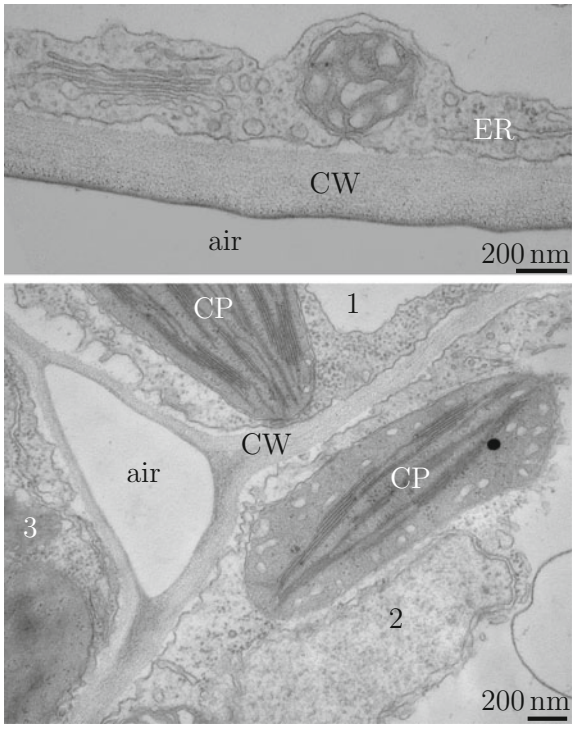

Fig. 10 Transmission electron microscopy images showing (top) cell walls (CW) and adjacent endoplasmic reticulum (ER) within the cell at the water/air interface and (bottom) intercellular air space and cell walls at the point of contact of three mesophyll cells (1, 2, 3) with chloroplasts (CP) in an *Arabidopsis thaliana* leaf

entering the symplasm of phloem and mesophyll cells water channels (aquaporins) have to be present, since the cell membrane consists of phospholipid bilayers that offer high resistance to water molecules.

Balance of water partitioning from xylem to evaporation, mesophyll uptake and phloem circulation is crucial for the adaption of plants to different growth conditions and climates. Indeed, the molecular biological removal of plasma membrane aquaporins in poplar by RNAi led to changes in the leaf shape, higher evaporation rates, larger stomatal opening and a restructuring of the cell wall as indicated by changes in gene expression for the respective membrane transporters and phytohormones (Bi et al. 2015). Binding of water molecules to the hydrophilic cellulose, hemicellulose and pectin compounds of the cell wall plays a large role at the cell wall–intercellular space interface. Evaporation will lead to an increasingly negative pressure between the structural cell wall compounds at the interface. This negative pressure is assumed to pull the water from the xylem to the evaporating cell wall surface in the mesophyll (Taiz and Zeiger 2010), i.e. a quite long distance in the range of 50–300 µm, including passage of the bundle sheath. It is unclear, though, how these events on the surface of the cell wall translate to the inner layers of the 200–500 nm thick mesophyll cell wall (Fig. 10) which abuts the plasma membrane. Under drought conditions, their aquaporins are closed ('gated') in order to limit the intracellular water loss, which would lead to loss of turgor of the mesophyll cells and,

thus, leaf wilting (Törnroth-Horsefield et al. 2006). The question to be raised here is how the evaporation-generated water tension in the cell wall of a given mesophyll cell translates into the negative pressure in xylem vessels. It is suggestive to postulate an unbroken apoplasmic water continuum between mesophyll and xylem, necessary to pull water up into the leaves. The evaporation-generated water loss in the mesophyll will however also have a direct influence on the water content in the mesophyll cells as long as aquaporins are open. It is also conceivable that the intracellular water content of mesophyll cells is supplied for via the symplasmic pathway, i.e. plasmodesmata between the bundle sheath and the mesophyll (Fig. 7). A pivotal role of the bundle sheath for water export from the vascular bundles and sugar import into vascular bundles is given in plant taxa that have an endodermis-like bundle sheath, as, e.g. the gymnosperms (Liesche et al. 2011). Here, water from the xylem has to cross the plasma membrane of the bundle sheath and might well be transported on symplasmically, i.e. through plasmodesmata (Schulz 2015).

Pre-phloem Pathways of Sugars

Evolution of the long-distance transport of assimilates has led to three different strategies of phloem loading, two active ones and a passive one. The active ones involve an accumulation of sugars in the sieve element–companion cell complex, and consumption of energy. By contrast, the passive one does not show accumulation of sugars in the phloem, but has the highest sugar concentration in the mesophyll. While the active apoplasmic strategy is characterized by an isolated phloem configuration with few if any plasmodesmata between the sieve element–companion cell complex and the bundle sheath, both symplasmic strategies depend upon phloem cells which are well coupled to the bundle sheath via plasmodesmata (Fig. 11). The pathway from the mesophyll to the bundle sheath, and where existent, further to the phloem parenchyma (pre-phloem pathway), is symplasmic for any loading strategy, i.e. bound to plasmodesmata (Schulz 2015).

Mechanistically, the apoplasmic loading mode is the easiest to understand. Since the sieve element–companion cell complexes are symplasmically isolated, they can accumulate sugar without leakage—once in, it can only follow the sieve tube systems towards the sinks. The interesting interface for this strategy which is most established in herbs is the wall isolating the sieve element–companion cell complex from neighbouring cells such as the bundle sheath. For the release of sucrose, the main transport sugar in those plant families, there are membrane transport proteins of the SWEET type allowing facilitated diffusion. Release through theses permeases is downhill and does not require energy (Chen et al. 2012). Sucrose in the apoplasmic interface between bundle sheath and complex has then to be actively taken up by sucrose-proton cotransporters called SUTs that are indirectly fuelled by ATP hydrolysis driving the plant proton pump. Both membrane steps involved, facilitated diffusion from the bundle sheath into the apoplast and active uptake into the phloem, are saturable and mainly depend on their respective maximal reaction rate V_{max} and

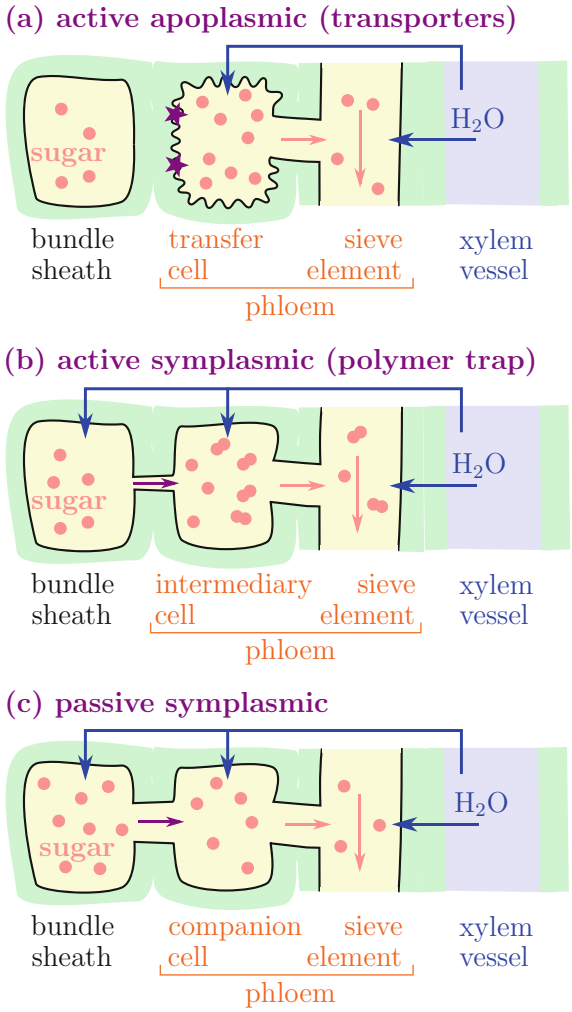

Fig. 11 The three known modes of sugar loading into the phloem and possible water pathways. **a** In active apoplasmic loading, sugars are taken up from the apoplast (cell wall space) into transfer cells with the help transporter proteins. Water can enter the transporting sieve elements either directly from the xylem or via the transfer cells. **b** In active symplasmic loading, the sugar uptake from bundle sheath into intermediary cell happens via the symplast. The loading mode is considered active due to the enzymatic transformation of sucrose to larger sugar molecules, like raffinose and stachyose, inside the intermediary cell. The larger sugars are thereby trapped inside the phloem, which facilitates an increased sugar concentration in the phloem. The trapping is only possible, because the symplasmic connections (plasmodesmata) between bundle sheath and intermediary cell are very narrow in this loading mode. Compared to apoplasmic loading, water can additionally enter the phloem symplasmically through these narrow plasmodesmata. **c** In passive symplasmic loading, sugar follows a downhill gradient from bundle sheath into the phloem. All cells are well connected with plasmodesmata

number per membrane area. It can be postulated that the high sucrose concentration in the sieve element–companion cell complex osmotically attracts water which can move in through aquaporins. While there are calculations available for the V_{max} of the sucrose transporter proteins (SWEETs and SUC2/SUT1), their density in the plasma membrane is not determined yet (Chen et al. 2012; Sauer 2007; Kühn and Grof 2010). Neither is the distribution of aquaporins in the sieve element–companion cell complex or their gating behaviour assessed (see Schulz 2015). It is far from trivial to keep track of the water being co-transported by the active sugar transporter. Many membrane pumps carry water through the membrane in addition to their target 'substrate' molecule. In this way, water can move against chemical potential gradients of substantial size as seen, e.g. in the intestinal sodium/glucose cotransporter SGLT1 (Zeuthen et al. 2016) as shown pictorially in Fig. 12.

In active symplasmic loading, sugars can move symplasmically from the bundle sheath into the sieve element–companion cell complex. In the intermediary cells (as the companion cells are called in this loading mode) enzymes convert sucrose into sugar oligomers, like raffinose and stachyose. These oligomers are then trapped inside the phloem due to the fact that they are slightly larger than sucrose and that the plasmodesmal pores between bundle sheath cell and intermediary cell are very narrow. This is why the mechanism is also called the *polymer trap*. In contrast to the apoplasmic loading, water can in this mechanism also enter the phloem from the bundle sheath through the plasmodesmata. This bulk flow of water even contributes to the loading of sugars into the phloem, so that the uptake of sugars is not purely diffusive, but also partly advective.

With respect to water uptake and pathways the third loading mode—passive symplasmic loading—is quite similar to the polymer trap. The main differences to the polymer trap case are wider plasmodesmata between bundle sheath and companion

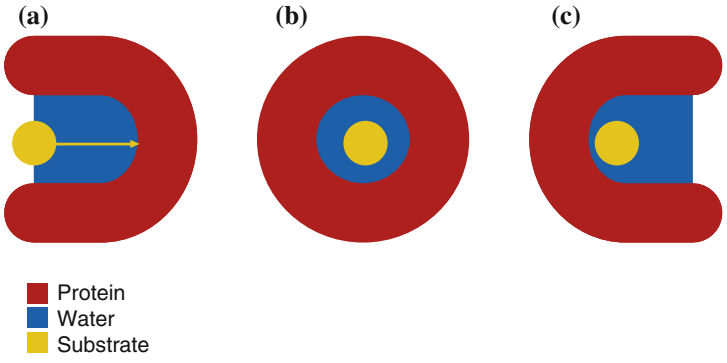

Fig. 12 Cartoon of a membrane protein that co-transports water in the process of pumping the substrate molecule shown in yellow. There will be a net water transport if some water is expelled after step (c), which can occur, e.g. by conformational changes of the protein. This mechanism allows for 'uphill' water transport—against a pressure gradient or a water concentration (osmotic) gradient. From Zeuthen and MacAulay (2012)

cells, and no enzymatic sugar conversion in the passive symplasmic loading mode. The concentration of sugars is highest in the mesophyll cells and sugars follow a downhill gradient into the phloem, in contrast to both active loading modes.

Mathematically the flux of water and of sugar through plasmodesmata can be described by the Kedem–Katchalsky equations (Kedem and Katchalsky 1958):

$$J_V = L_p(\Delta p - \sigma RT\Delta c) \tag{17}$$

$$j_s = \omega RT\Delta c + (1-\sigma)\bar{c}J_V, \tag{18}$$

where $\bar{c}$ is the mean solute concentration, ω is the mobility of the solute and σ is the reflection coefficient. (17) contains two causes for the movement of water: a hydrostatic pressure potential Δp or a difference in osmotic potential $RT\Delta c$. According to (18), sugar is advected with the bulk volume flow J_V, and diffusing due to the difference in sugar concentration. Here J_V is a flux pr. area with SI unit $m^3\ s^{-1}\ m^{-2} = m\ s^{-1}$ (as a velocity) composed of

$$J_V = j_w\bar{v}_w + j_s\bar{v}_s, \tag{19}$$

where j_w and j_s are molar fluxes of water and solutes, respectively, with SI unit mol $s^{-1}\ m^{-2}$, and $\bar{v}_w$ and $\bar{v}_s$ are the corresponding molar volumes. In situations where the solute concentrations are low, it is usually a good approximation to replace J_V with the water part $j_w\bar{v}_w$, an approximation which is often made.

The meaning of reflection coefficient σ and mobility ω can be best understood by thinking of the porous interface as a membrane. If this membrane is ideally semipermeable, then $\sigma = 1$ and $\omega = 0$, meaning that the solute size is larger than the pore diameter and the solute cannot pass through the pore. In the other extreme, the pores are much larger than the solute, implying that $\sigma = 0$ and ω is directly proportional to the free diffusion coefficient ($\omega = \frac{A}{dRT}D_{\text{free}}$, with A and d the area and thickness of the membrane, and assuming a constant concentration gradient).

The challenge in understanding the polymer trap loading mechanism is that the plasmodesmatal pores should be extremely selective. Indeed, they should let sucrose through without too much trouble, but they should stop raffinose and stachyose, although the hydrodynamic radius of a raffinose molecule is only 25% larger than sucrose molecules. It is well known that the plasmodesmata connecting the companion cell to the bundle sheath are unusually narrow and branched towards the companion cell end. In addition, the endoplasmic reticulum (ER), which permeates the plasmodesmata, makes the estimate of the available space for transport very uncertain (Volk et al. 1996; Fisher and Gifford 1986; Waigmann et al. 1997). Aside from partially blocking the plasmodesmata, the role of the ER is not well understood. Recently, Nixon-Abell et al. (2016) have obtained spectacular views of the packed tubular arrays of the ER inside animal cells, and it is obvious that many important functions could be carried out within these structures—something which remains to be explored.

Some progress has been made in using simple models of the unblocked part of the plasmodesmata through which the fluid can flow to study the sugar/water transport (Dölger et al. 2014; Comtet et al. 2017). In Waigmann et al. (1997), it was suggested to model them as circular slits with half-width around 1 nm, as shown in Fig. 13, and this suggestion is followed in Dölger et al. (2014).

With this geometry, one can estimate the parameters in the Kedem–Katchalsky equations as

$$\omega = n_{\mathrm{PD}} \frac{4\pi r_{\mathrm{PD}} h}{dRT} H(r_{\mathrm{solute}}/d) D_{\mathrm{cyt}}, \tag{20}$$

where, from the Einstein relation, the molecular diffusivity outside of the pores is

$$D_{\mathrm{cyt}} \approx \frac{kT}{6\pi\eta r_{\mathrm{solute}}} \tag{21}$$

and $H(\lambda = r_{\mathrm{solute}}/d)$ is a 'hindrance factor' for passage through a narrow tube (Dechadilok and Deen 2006).

Similarly, the membrane permeability is

$$L_p \approx n_{\mathrm{PD}} \frac{4\pi r_{\mathrm{PD}} h^3}{3\eta d} \tag{22}$$

and with similar estimates for the 'convective' hindrance factor $W(\lambda) = 1 - \sigma$ (Dechadilok and Deen 2006), one can compute the water and solute fluxes for given concentration gradients. Inside the pores one can decompose the solute flux into a diffusive and a convective part:

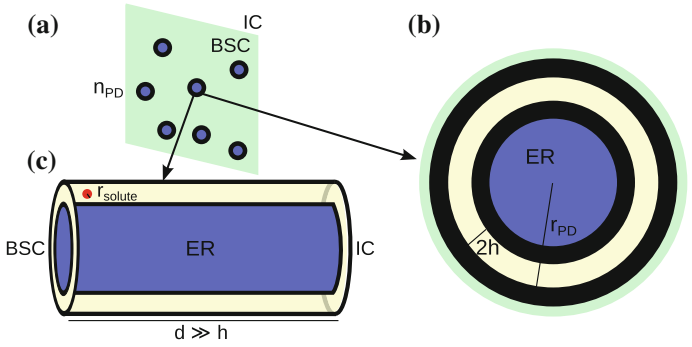

Fig. 13 A possible structure for a plasmodesmal pore: slit pores as suggested by Waigmann et al. (1997). **a** Part of the cell wall between the bundle sheath (BSC) and the intermediary cell (IC) with plasmodesmata (PD) density n_{PD}. **b** The assumed substructure of a PD shown in cross section and **c** in three-dimensional view. The cytoplasmic sleeve (light yellow) available for water and sugar transport is restricted by the desmotubule of the endoplasmic reticulum (ER, blue) and electron-dense particles (black) attached to the membrane, and is assumed to take the form of a circular slit with radius r_{PD}, half-width h and length d. From Dölger et al. (2014)

$$j_s = -D\frac{\partial c}{\partial x} + uc, \tag{23}$$

where, comparing to (18), $u = (1-\sigma)J_V$ and $D \approx \omega RTd$ for a pore with length d. Finally, sugar conservation gives

$$\frac{\partial c}{\partial t} = -\nabla \cdot j_s = -\frac{\partial j_s}{\partial x} \tag{24}$$

and for the stationary case, where $\frac{\partial c}{\partial t} = \frac{\partial j_s}{\partial x} = 0$, j_s is constant. The linear relation between solute flux j_s and concentration differences Δc in (18) assumes that the Peclet number $\mathrm{Pe} = ud/D = d(1-\sigma)J_V/D$ is small. In general, one can simply solve (23) for c with constant j_s, i.e.

$$\frac{\partial c}{\partial s} = \mathrm{Pe}\ c - n, \tag{25}$$

where $n = j_s d/D$ and s is the scaled variable $s = x/d$. The solution with $c(x = 0) = c_0$ and $c(x = d) = c(s = 1) = c_1$ is

$$\frac{c(s)}{c_0} = \left(1 - \frac{n}{\mathrm{Pe}}\right) e^{s\mathrm{Pe}} + \frac{n}{\mathrm{Pe}} \tag{26}$$

giving

$$\frac{c_1}{c_0} = \left(1 - \frac{n}{\mathrm{Pe}}\right) e^{\mathrm{Pe}} + \frac{n}{\mathrm{Pe}} \tag{27}$$

so that we can express $j_s = nD/d$ in terms of the concentrations on the two sides of the membrane as

$$j_s = (1-\sigma)J_V\left(c_0 + \frac{\Delta c}{e^{\mathrm{Pe}} - 1}\right), \tag{28}$$

where $\Delta c = c_0 - c_1$. For small Pe, this reduces to

$$j_s \approx (1-\sigma)J_V c_0 + \frac{D}{d}\Delta c \tag{29}$$

in agreement with (18) with c_0—the 'upwind' concentration—replacing $\bar{c}$. This approach was used in Comtet et al. (2017), who also included a description of the enzymatic reaction oligomerizing the sugars. As one can see, the effect of including large values of Pe (or small values of D) in (28) is very small since $\mathrm{Pe} \gg 1$ leads to

$$j_s \approx (1-\sigma)J_V c_0 + (1-\sigma)J_V e^{-\mathrm{Pe}}\Delta c, \tag{30}$$

where the diffusive contribution is exponentially small. Indeed, the conclusions of Dölger et al. (2014) and of Comtet et al. (2017) are quite compatible. To avoid the oligomers (in particular raffinose) from flowing back into the bundle sheath, the slit

half-width has to be less than around 6.0 Å, but to allow sucrose to flow through it has to be larger than around 4.2 Å. For molecules (sucrose) passing such very narrow tubes, the theory summarized in Dechadilok and Deen (2006) for the hindrance factors $H(\lambda)$ and $W(\lambda)$ is at the limit of its validity—in addition to the fact that the molecules are treated as spherical. If these approximations are used anyway, it is found that it is possible to get enough sugar through, and in addition (Dölger et al. 2014) that enough water will likely follow along with this sugar flow to drive the phloem, and thus, that no additional water intake is needed through aquaporins in the membranes. It is also remarked that efficient blocking of raffinose will only take place when the pores are very close to the 5.2 Å. One might have speculated that the water current was sufficiently strong to keep out the raffinose of even larger pores, but this does not seem feasible, at least with the parameters coming from *Cucumis melo*. In Comtet et al. (2017), it is speculated that *some* backflow of raffinose might actually occur, since it might be degraded once it reaches the bundle sheath. This might indeed be so, but even with the very narrow pores assumed in Dölger et al. (2014), the sucrose flow rate seems substantially larger than observed in *Cucumis melo* (Schmitz et al. 1987). This might be due to the very complicated and mostly unknown structure and function of the ER as alluded to above.

Conclusion

In this short review, we have tried to present an overview of essential points in the current knowledge and mode of description of the coupling of water motion and sugar translocation in leaves—both in the sieve tubes of the veins, where the sugar is transported to the rest of the plant, and through the pre-phloem pathway that leads from the sugar producing mesophyll cells via the bundle sheath to the sieve cells. The challenges in understanding the full circuit of water in the leaf are considerable. From the xylem tubes inside the vascular bundle where water exits the vascular system, most of it will evaporate out through the stomata in the leaf surface, but a small amount has to be left behind, and take part in the photosynthetic sugar production and the subsequent sugar transport. Presumably, the large negative pressures, dragging the water all the way up to the leaves, originate in the cell walls of the mesophyll, and thus, the mesophyll cells must be able to balance the water potential very delicately, so that enough water is retained to carry out these tasks. Being part of the pre-phloem, the mesophyll cells are believed to typically have positive pressures (turgor) inside and this means that they have to be able to create very large water potential gradients from high concentrations of solutes. How this is done, and how it plays together with the different loading mechanisms, is not known in detail. When plasmodesmata are important for the sugar translocation, they obviously have to be able to conduct sugar efficiently enough while presumably keeping out many other similarly sized (or even smaller) molecules which the cell wants to keep. How this is done is not known, but very likely the endoplasmic reticulum plays an important role to be explored in the future.

References

Bi Z, Merl-Pham J, Uehlein N, Zimmer I, Mühlhans S, Aichler M, Walch AK, Kaldenhoff R, Palme K, Schnitzler J-P, Block K (2015) RNAi-mediated downregulation of poplar plasma membrane intrinsic proteins (PIPs) changes plasma membrane proteome composition and affects leaf physiology. J Proteomics 128:321–332

Carvalho MR, Turgeon R, Owens T, Niklas KJ (2017a) The hydraulic architecture of ginkgo leaves. Am J Bot 104(9):1285–1298

Carvalho MR, Turgeon R, Owens T, Niklas KJ (2017b) The scaling of the hydraulic architecture in poplar leaves. New Phytol 214:145–157

Chen L-Q, Qu X-Q, Hou B-H, Sosso D, Osorio S, Fernie AR, Frommer WB (2012) Sucrose efflux mediated by sweet proteins as a key step for phloem transport. Science 335(6065):207–211

Comtet J, Turgeon R, Stroock AD (2017) Phloem loading through plasmodesmata: a biophysical analysis. Plant Physiol 175(2):904–915

Dechadilok P, Deen WM (2006) Hindrance factors for diffusion and convection in pores. Ind Eng Chem Res 45(21):6953–6959

Dölger J, Rademaker H, Liesche J, Schulz A, Bohr Tomas (2014) Diffusion and bulk flow in phloem loading: a theoretical analysis of the polymer trap mechanism for sugar transport in plants. Phys Rev E 90(4):042704

Fisher DB, Gifford RM (1986) Accumulation and conversion of sugars by developing wheat grains vi. gradients along the transport pathway from the peduncle to the endosperm cavity during grain filling. Plant Physiol 82(4):1024–1030

Jensen KH, Berg-Sørensen K, Bruus H, Holbrook NM, Liesche J, Schulz A, Zwieniecki MA, Bohr T (2016) Sap flow and sugar transport in plants. Rev Mod Phys 88:035007 (1–63)

Jensen KH, Lee J, Bohr T, Bruus H, Holbrook NM, Zwieniecki MA (2011) Optimality of the Münch mechanism for translocation of sugars in plants. J R Soc Interface 8(61):1155–1165

Jensen KH, Berg-Sørensen K, Friis SMM, Bohr T (2012a) Analytic solutions and universal properties of sugar loading models in münch phloem flow. J Theor Biol 304:286–296

Jensen KH, Liesche J, Bohr T, Schulz A (2012b) Universality of phloem transport in seed plants. Plant Cell Environ 35:1065–1076

Jensen KH, Mullendore DL, Holbrook NM, Bohr T, Knoblauch M, Bruus H (2012c) Modeling the hydrodynamics of phloem sieve plates. Front Plant Sci 3

Jensen KH, Zwieniecki MA (2013) Physical limits to leaf size in tall trees. Phys Rev Lett 110(1)

Kedem O, Katchalsky A (1958) Thermodynamic analysis of the permeability of biological membranes to non-electrolytes. BBA—Biochim Et Biophys Acta 27:229–246

Knoblauch M, Knoblauch J, Mullendore DL, Savage JA, Babst BA, Beecher SD, Dodgen AC, Jensen KH, Holbrook NM (2016) Testing the Munch hypothesis of long distance phloem transport in plants. Elife 5

Kühn C, Grof CPL (2010) Sucrose transporters of higher plants. Curr Opin Plant Biol 13(3):287–297

Landsberg JJ, Fowkes ND (1978) Water movements through plant roots. Ann Bot 42:493–508

Liesche J, Martens HJ, Schulz A (2011) Symplasmic transport and phloem loading in gymnosperm leaves. Protoplasma 248(1):181–190

Liesche J, Windt C, Bohr T, Schulz A, Jensen KH (2015) Slower phloem transport in gymnosperm trees can be attributed to higher sieve element resistance. Tree Physiol (in press)

Lu SY, Zhao HY, Des Marais DL, Parsons EP, Wen XX, Xu XJ, Bangarusamy DK, Wang GC, Rowland O, Juenger T, Bressan RA, Jenks MA (2012) Arabidopsis eceriferum9 involvement in cuticle formation and maintenance of plant water status. Plant Physiol 159:930–944

Martens HJ (2017) Private correspondence

Niklas KJ (1994) Plant allometry: the scaling of plant form and process. University of Chicago Press

Nixon-Abell J, Obara CJ, Weigel AV, Li D, Legant WR, Xu CS, Pasolli HA, Harvey K, Hess HF, Betzig E, Blackstone C, Lippincott-Schwartz J (2016) Increased spatiotemporal resolution reveals highly dynamic dense tubular matrices in the peripheral ER. Science 354, aaf3928–1–12

Rademaker H (2016) Microfluidics of sugar transport in plant leaves and in biomimetic devices. PhD thesis, Technical University of Denmark
Rademaker H, Jensen KH, Bohr T (2016) Osmotically driven flows and maximal transport rates in systems of long, linear porous pipes. arXiv:1610.09175
Rademaker H, Zwieniecki MA, Bohr T, Jensen KH (2017) Sugar export limits size of conifer needles. Phys Rev E 95:042402
Ronellenfitsch H, Liesche J, Jensen Kaare H, Holbrook NM, Schulz A, Katifori E (2015) Scaling of phloem structure and optimality of photoassimilate transport in conifer needles. In: Proceedings of the royal society of london B: biological sciences, vol 282(1801)
Sauer N (2007) Molecular physiology of higher plant sucrose transporters. FEBS Lett 581(12):2309–2317
Schmitz K, Cuypers B, Moll M (1987) Pathway of assimilate transfer between mesophyll-cells and minor veins in leaves. Cucumis melo L. Planta 171(1):19–29
Schulz A (2015) Diffusion or bulk flow: how plasmodesmata facilitate pre-phloem transport of assimilates. J Plant Res 128(1):49–61
Tadrist L, Darbois-Texier B (2016) Are leaves optimally designed for self-support? an investigation on giant monocots. J Theor Biol 396:125–131
Taiz L, Zeiger E (2010) Plant physiology, 5th edn. Sinauer Associates Inc, Sunderland, MA
Törnroth-Horsefield S, Wang Y, Hedfalk K, Johanson U, Karlsson M, Tajkhorshid E, Neutze R, Kjellbom P (2006) Structural mechanism of plant aquaporin gating. Nature 439:688–694
Volk GM, Turgeon R, Beebe DU (1996) Secondary plasmodesmata formation in the minor-vein phloem. Cucumis Melo L and Cucurbita pepo L Planta 199(3):425–432
Waigmann E, Turner A, Peart J, Roberts K, Zambryski P (1997) Ultrastructural analysis of leaf trichome plasmodesmata reveals major differences from mesophyll plasmodesmata. Planta (Heidelberg) 203(1):75–84
Zeuthen T, Gorraitz E, Her K, Wright EM, Loo DDF (2016) Structural and functional significance of water permeation through cotransporters. Proc Nat Acad Sci (USA) 113(44):E6887–E6894
Zeuthen T, MacAulay N (2012) Transport of water against its concentration gradient: fact or fiction? WIREs membr transp signal 2012. https://doi.org/10.1002/wmts.54